The Fourier-series method for calculating strain distributions in two dimensions

1997 J. Phys.: Condens. Matter 9 4509

(http://iopscience.iop.org/0953-8984/9/22/004)

J. Phys.: Condens. Matter **9** (1997) 4509–4520. Printed in the UK PII: S0953-8984(97)79048-9

The Fourier-series method for calculating strain distributions in two dimensions

J R Downes and D A Faux

Physics Department, University of Surrey, Guildford, Surrey, GU2 5XH, UK

Received 30 October 1996, in final form 13 March 1997

Abstract. The Fourier-series method for calculating strain distributions within a rectangular isotropic elastic block is extended to allow boundary conditions which may include normal or shear stress components. The method is then further extended to include boundary conditions expressed as displacements allowing, in principle, the evaluation of strain fields in device structures with more complex geometries. This extension provides an alternative strain evaluation technique for two-dimensional structures which can be described as a system of linked rectangular elastic blocks. The method is illustrated by calculating the strain field for a transmission electron microscopy sample in which a strained layer meets the free surfaces at an angle of 45°.

1. Introduction

The presence of strain and the relaxation of strain have a number of interesting and well documented effects on the electronic and mechanical properties of semiconductor structures and have promoted significant interest in the calculation of strain fields in a broad range of semiconductor device structures [1]. For instance, knowledge of the strain fields in quantum wells are required because strain leads to modifications of the band structure and may induce piezoelectricity in certain devices. The determination of strain relaxation in strained quantum wires is a necessary precursor to calculations of their electronic properties [2–4]. Calculation of strain fields enables an assessment to be made of possible mechanical problems in devices. For example, strains caused during bonding to heat sinks can lead to early degradation of lasers [5]. Strain calculations also form an integral part of some experimental techniques. The measurement of strain in semiconductor devices by, for example, examining contrast patterns obtained by transmission electron microscopy (TEM) requires a theoretical determination of the strain fields near the edge of such structures to enable proper interpretation of the images [6–8].

Calculations of strain distributions in strained-layer semiconductor structures first appeared in the late 1970s, at the time the first high-quality strained layers were grown. Finite-element analysis, developed for the engineering world, has been applied by several groups [3, 4, 9, 10]. One significant advantage of finite-element analysis is that it can be used to treat problems with complex geometries. Unfortunately, this advantage is offset because many strained-layer or strained quantum-wire structures are long and thin with high aspect ratios and the subsequent demands on computing resources (principally large memory requirements) make certain calculations difficult. In some cases, the boundary-element method would be the preferred strain evaluation technique because the boundary

0953-8984/97/224509+12$19.50

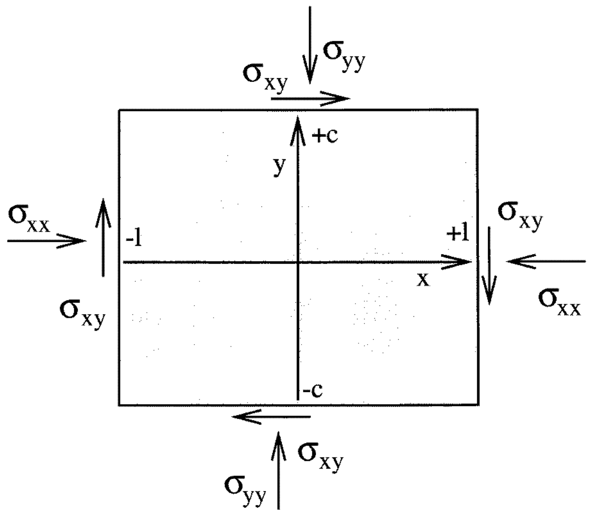

Figure 1. An elastic block subjected to normal and tangential tractions on all four sides.

of the structure instead of its volume is discretized, but this advantage comes at the cost of increased mathematical complexity [11]. Commercial packages are not yet widely available which means the complex mathematics must be performed by the individual.

In this environment many authors have presented analytic methods of calculating strain fields for particular structures [12–30]. Usually the focus is on one aspect of the strain field. For example, several authors have studied the bending moments in stacks of strained layers, but have ignored the relaxation at the ends of the layers. Also, calculations which are not rigorously correct have been presented. For example, the concentrated-point-force model, and the subsequent distributed-force model of Hu [24, 25] for calculating the stress distributions at the edge of a strained film are approximations and the stress fields presented do not obey the equilibrium conditions of linear elasticity. Analytic results are nevertheless useful because they allow quick calculations of strain components at any point and may yield simple functional forms in certain limits.

The Fourier-series method, on which the present paper focuses, has all the advantages of analytic methods and the ability to treat high-aspect-ratio structures, although the theory is currently restricted to isotropic materials. The analysis presented by Faux and Haigh [15] in 1990 developed from the work of Pickett [31] and Timoshenko and Goodier [32] but only permitted normal stress components to be specified on the top and bottom surfaces of an infinite layer. In 1994, Faux [16] extended the analysis to allow normal stress components on the left and right surfaces as well as the top and bottom surfaces of a finite rectangular block. Faux and Gill [17] subsequently presented a three-dimensional analysis for symmetrical normal stress components on a cuboid. The analysis presented here extends this earlier work and allows boundary conditions of shear and normal forces on all boundaries to be specified.

The generalization of the Fourier-series method to include tangential surface forces is presented in section 2. An extension of the theory to treat a system of connected blocks is discussed in section 3. Results for the strain distribution of a TEM sample are presented in section 4 and conclusions follow in section 5.

2. Theory

The Airy stress function [32] ϕ for isotropic materials in two dimensions must satisfy the differential equation

$$\nabla^4\phi = \frac{\partial^4\phi}{\partial x^4} + 2\frac{\partial^4\phi}{\partial x^2\partial y^2} + \frac{\partial^4\phi}{\partial y^4} = 0 \qquad (1)$$

and the stress components are then obtained from ϕ using

$$\sigma_{xx} = \frac{\partial^2\phi}{\partial y^2} \qquad \sigma_{yy} = \frac{\partial^2\phi}{\partial x^2} \qquad \text{and} \qquad \sigma_{xy} = -\frac{\partial^2\phi}{\partial x\partial y}. \qquad (2)$$

The Fourier-series method [15–17] relies on choosing an Airy stress function which gives stresses at the boundaries of a rectangular block in the form of a Fourier series. Choice of the stress function is the most important aspect of the method and in its most general form, for the two-dimensional rectangular block shown in figure 1, the stress function should be

$$\begin{aligned}\phi(x, y) = \frac{1}{2}\sigma_{XX}y^2 + \frac{1}{2}\sigma_{YY}x^2 - \sigma_{XY}xy + \sum_{i=1}^{\infty} A_i^{\pm}\cos\alpha_i x h_i^{\pm}(y) + B_i^{\pm}\sin\alpha_i' x h_i^{'\pm}(y)\\ - \sum_{i=1}^{\infty} C_i^{\pm}\sin\alpha_i x i_i^{\pm}(y) - D_i^{\pm}\cos\alpha_i' x i_i^{'\pm}(y)\\ + \sum_{i=1}^{\infty} E_i^{\pm}\cos\beta_i y j_i^{\pm}(x) + F_i^{\pm}\sin\beta_i' y j_i^{'\pm}(x)\\ - \sum_{i=1}^{\infty} G_i^{\pm}\sin\beta_i y k_i^{\pm}(x) - H_i^{\pm}\cos\beta_i' y k_i^{'\pm}(x) \qquad (3)\end{aligned}$$

where α_i, α_i', β_i and β_i' are Fourier frequencies and A_i, B_i, C_i, D_i, E_i, F_i, G_i and H_i are constants which will be referred to as the Fourier coefficients of the stress function. The functions $h_i(y)$, $i_i(y)$, $j_i(x)$, $k_i(x)$, $h_i'(y)$, etc will be referred to as fitting functions. The functions $h_i^{+}(y)$ and $h_i^{'+}(y)$ are different functions, each being associated with either the cosine or sine terms of the Fourier series. Differentials will be distinguished by primes appearing after the '$\pm$' superscripts. The superscript '$\pm$' indicates that each line represents two sums, one where the constants and functions have positive superscripts and one where they have negative superscripts. These refer to terms which can be associated with the upper and lower, or left and right, surfaces of the block, respectively. On differentiation, the first three terms, σ_{XX}, σ_{YY} and σ_{XY}, become the zeroth-order term of the Fourier series for the three stresses σ_{xx}, σ_{yy} and σ_{xy}. Note that the unusual ordering of the trigonometric functions in the four sums means that the usual ordering is obtained when equations (2) are used to obtain the stresses by differentiation.

Faux and Haigh [15] only included the first sum of the stress function (that involving the coefficients A and B) and so included only normal forces on the top and bottom surfaces of an infinite layer. Faux [16] extended the analysis to include the third sum (involving the E and F coefficients) which allowed normal forces on the left and right surfaces as well as the top and bottom surfaces of a finite rectangular block. The following analysis includes all terms of equation (3) allowing boundary conditions specifying shear stress to be included. The choice of the Fourier frequencies and the fitting functions will determine the detail of the mathematics, but in all cases a set of Fourier coefficients of the stress function which yield stresses satisfying the specified boundary conditions is required.

The stress function must be a solution of equation (1) and, by substitution, the following form for the fitting functions $h_i^{\pm}(y)$ can be deduced:

$$h_i^{\pm}(y) = \mathrm{h}_{C1i}^{\pm} \cosh \alpha_i y + \mathrm{h}_{C2i}^{\pm} \sinh \alpha_i y + \mathrm{h}_{C3i}^{\pm} y \cosh \alpha_i y + \mathrm{h}_{C4i}^{\pm} y \sinh \alpha_i y \tag{4}$$

where $\mathrm{h}_{C1i}^{\pm}$, $\mathrm{h}_{C2i}^{\pm}$, $\mathrm{h}_{C3i}^{\pm}$, $\mathrm{h}_{C4i}^{\pm}$ are arbitrary constants. Similar expressions for $i_i^{\pm}(y)$, $j_i^{\pm}(y)$ and $k_i^{\pm}(y)$, and the primed functions can be found. The four arbitrary constants of the eight sets of fitting functions can be chosen to simplify the mathematics.

The stress obtained from the stress function using equation (2) must equal the specified stress components at each boundary. For example, $\sigma_{xx}(x, y)$ is given by

$$\begin{aligned}\sigma_{xx}(x, y) = \sigma_{XX} &+ \sum_{i=1}^{\infty} A_i^{\pm} \cos \alpha_i x h_i^{\pm''}(y) + B_i^{\pm} \sin \alpha_i' x h_i^{'\pm''}(y) \\ &- \sum_{i=1}^{\infty} C_i^{\pm} \sin \alpha_i x i_i^{\pm''}(y) - D_i^{\pm} \cos \alpha_i' x i_i^{'\pm''}(y) \\ &- \sum_{i=1}^{\infty} E_i^{\pm} \beta_i^2 \cos \beta_i y j_i^{\pm}(x) + F_i^{\pm} \beta_i^{'2} \sin \beta_i' y j_i^{'\pm}(x) \\ &+ \sum_{i=1}^{\infty} G_i^{\pm} \beta_i^2 \sin \beta_i y k_i^{\pm}(x) - H_i^{\pm} \beta_i^{'2} \cos \beta_i' y k_i^{'\pm}(x)\end{aligned} \tag{5}$$

and by setting $x = +l$ the normal stress at the right-hand surface of the elastic block can be obtained:

$$\begin{aligned}\sigma_{xx}(l, y) = \sigma_{XX} &+ \sum_{i=1}^{\infty} A_i^{\pm} \cos \alpha_i l h_i^{\pm''}(y) + B_i^{\pm} \sin \alpha_i' l h_i^{'\pm''}(y) \\ &- \sum_{i=1}^{\infty} C_i^{\pm} \sin \alpha_i l i_i^{\pm''}(y) - D_i^{\pm} \cos \alpha_i' l i_i^{'\pm''}(y) \\ &- \sum_{i=1}^{\infty} E_i^{\pm} \beta_i^2 \cos \beta_i y j_i^{\pm}(l) + F_i^{\pm} \beta_i^{'2} \sin \beta_i' y j_i^{'\pm}(l) \\ &+ \sum_{i=1}^{\infty} G_i^{\pm} \beta_i^2 \sin \beta_i y k_i^{\pm}(l) - H_i^{\pm} \beta_i^{'2} \cos \beta_i' y k_i^{'\pm}(l).\end{aligned} \tag{6}$$

This stress can be set equal to the boundary stress, which gives an equation relating all of the unknown Fourier coefficients of the stress function to the known Fourier coefficients of the normal stress imposed on the right-hand surface. For example, suppose the boundary condition for the normal stress on the right-hand surface, when expressed as a Fourier series, is

$$\sigma_{xx}(l, y) = \sigma_{XX} + \sum_{i=1}^{\infty} W_i^{+} \cos \beta_i y + X_i^{+} \sin \beta_i y. \tag{7}$$

Multiplying equations (6) and (7) by $\cos \beta_i y$ and integrating with respect to y from $-c$ to $+c$, enables terms of equal frequency to be equated. The following relationship then holds for the W_r^{+},

$$
\begin{aligned}
W_r^+ c = \sum_{i=1}^{\infty} A_i^{\pm} \cos\alpha_i l \int_{-c}^{+c} h_i^{\pm''}(y)\cos\beta_r \, \mathrm{d}y + B_i^{\pm} \sin\alpha_i' l \int_{-c}^{+c} h_i^{'\pm''}(y)\cos\beta_r \, \mathrm{d}y \\
- \sum_{i=1}^{\infty} C_i^{\pm} \sin\alpha_i l \int_{-c}^{+c} i_i^{\pm''}(y)\cos\beta_r \, \mathrm{d}y - D_i^{\pm}\cos\alpha_i' l \int_{-c}^{+c} i_i^{'\pm''}(y)\cos\beta_r \, \mathrm{d}y \\
-\{E_r^{\pm}\beta_r^2 j_r^{\pm}(l) - G_r^{\pm}\beta_r^2 k_r^{\pm}(l)\}c \qquad (8)
\end{aligned}
$$

where the subscripts i and r are integers. W_r^+ is the rth cosine Fourier coefficient of the normal stress on $x = +l$ and $A_i^{\pm}$, $B_i^{\pm}$, $C_i^{\pm}$, $D_i^{\pm}$, $E_r^{\pm}$ and $G_r^{\pm}$ are Fourier coefficients of the stress function.

It is possible to derive a total of 16 sets of equations of this type, involving each of the 16 Fourier coefficients of the boundary conditions, $A_i^{\pm}$, $B_i^{\pm}$, $C_i^{\pm}$, etc. If the summation over i is truncated, then equation (8) represents a large but finite number of simultaneous equations which can be solved by iterative techniques for the Fourier coefficients of the stress function.

A sensible choice of the Fourier frequencies and the fitting functions can simplify equations (8). This is illustrated by considering the shear stress. The shear stress is obtained from the stress function using equation (2),

$$
\begin{aligned}
\sigma_{xy}(x,y) = \sigma_{XY} + \sum_{i=1}^{\infty} \alpha_i A_i^{\pm} \sin\alpha_i x h_i^{\pm'}(y) - \alpha_i' B_i^{\pm}\cos\alpha_i' x h_i^{'\pm'}(y) \\
- \sum_{i=1}^{\infty} \alpha_i C_i^{\pm}\cos\alpha_i x i_i^{\pm'}(y) + \alpha_i' D_i^{\pm}\sin\alpha_i' x i_i^{'\pm'}(y) \\
+ \sum_{i=1}^{\infty} \beta_i E_i^{\pm}\sin\beta_i y j_i^{\pm'}(x) - \beta_i' F_i^{\pm}\cos\beta_i' y j_i^{'\pm'}(x) \\
- \sum_{i=1}^{\infty} \beta_i G_i^{\pm}\cos\beta_i y k_i^{\pm'}(x) + \beta_i' H_i^{\pm}\sin\beta_i' y k_i^{'\pm'}(x). \qquad (9)
\end{aligned}
$$

Table 1. Fourier frequencies that form basis sets.

	α_i	β_i	α_i'	β_i'
(1)	$i\pi/l$	$i\pi/c$	$i\pi/l$	$i\pi/c$
(2)	$i\pi/l$	$i\pi/c$	$\left(i-\frac{1}{2}\right)\pi/l$	$\left(i-\frac{1}{2}\right)\pi/c$
(3)	$\left(i-\frac{1}{2}\right)\pi/l$	$\left(i-\frac{1}{2}\right)\pi/c$	$i\pi/l$	$i\pi/c$

The Fourier frequencies must be chosen such that the trigonometric functions form a basis set, which allows at least the combinations shown in table 1. It was noted in an earlier work [16] that choosing the set of frequencies labelled (2) in table 1 produces an expression for the shear stress which involves no contribution from the first and third sums of the stress function. This, together with setting $C_i^{\pm}$, $D_i^{\pm}$, $G_i^{\pm}$ and $H_i^{\pm}$ equal to zero, gives a stress function in which the shear stress is zero at all four surfaces—a useful result if this is one of the boundary conditions. In the present case, the set of frequencies labelled (2) in table 1 are used and $G_i^{\pm}$ and $H_i^{\pm}$ are retained. If we now choose the fitting functions as follows,

$$i_i^{\pm'}(+l) = k_i^{-'}(+l) = 0 \qquad k_i^{+'}(+l) = -\frac{1}{\beta_i}$$
$$i_i^{'\pm'}(+l) = k_i^{'-'}(+l) = 0 \qquad \text{and} \qquad k_i^{'+'}(+l) = -\frac{1}{\beta_i}$$

then the shear stress at the boundary $x = +l$ reduces to the following form:

$$\sigma_{xy}(+l, y) = \sigma_{XY} + \sum_{i=1}^{\infty} G_i^+ \cos\beta_i y + H_i^+ \sin\beta_i' y. \tag{10}$$

This choice of frequencies and fitting functions means that the coefficients of the stress function, $G_i^\pm$ and $H_i^\pm$, are equal simply to the corresponding Fourier coefficients of the specified shear stress at the boundary $x = +l$. The $G_i^\pm$ and $H_i^\pm$ are, therefore, found immediately.

Equation (8) for the normal stresses can be reduced in a similar manner by a suitable choice of frequencies and fitting functions, but the reduction in this case is not so complete. Keeping to the frequencies chosen above and setting

$$j_i^+(+l) = -\frac{1}{\beta_i^2} \qquad j_i^-(+l) = 0 \qquad \text{and} \qquad k_i^\pm(+l) = 0$$

equation (8) reduces to

$$W_r^+ c = E_r^+ c + \sum_{i=0}^{\infty}(-1)^i \left\{ A_i^\pm \int_{-c}^{+c} h_i^{\pm''}(y)\cos\beta_i y\,\mathrm{d}y - B_i^\pm \int_{-c}^{+c} h_i^{'\pm''}(y)\cos\beta_i y\,\mathrm{d}y \right\}. \tag{11}$$

This time the Fourier coefficient E_r^+ is found in terms of W_r^+ and the Fourier coefficients $A_i^\pm$ and $B_i^\pm$. Provided a reasonable starting estimate is available, sets of equations similar to equation (11) can often be solved by cyclic iterative methods in which the starting estimate is progressively *relaxed* to the solution. This has been described in more detail in an earlier publication [16]. For instance, a sensible start is to set the coefficients $A_i^\pm$ and $B_i^\pm$ equal to zero so that

$$E_i^+ = W_i^+ \qquad E_i^- = W_i^- \qquad F_i^+ = X_i^+ \qquad \ldots. \tag{12}$$

These initial values for $E_i^\pm$ and $F_i^\pm$ may be used in equations similar to (11) to produce estimates for $A_i^\pm$ and $B_i^\pm$. These in turn can be used in equation (11) to produce improved estimates for $E_i^\pm$ and $F_i^\pm$. This iterative procedure is continued until all Fourier coefficients are known to the desired accuracy. Once the Fourier coefficients have been found, the stress components and hence the strains and displacements may be evaluated.

3. The Fourier-series method for linked elastic blocks

One of the primary limitations of the Fourier-series method is that the technique may only treat a single rectangular elastic block with a limited range of boundary conditions. To determine strain fields in device structures with complex geometries, such as strained overlayers [10] or buried strained layers, it is necessary to extend the Fourier-series method to link rectangular elastic blocks. This ability would greatly increase the range of structures accessible to the technique. For example, the strained overlayer, shown in figure 2, can be modelled as four distinct, but linked, elastic blocks with appropriate boundary and interface conditions. There exists continuity of normal and shear stress, normal and shear strain, and displacement for any surface through a continuous elastic medium (across BI or EH in

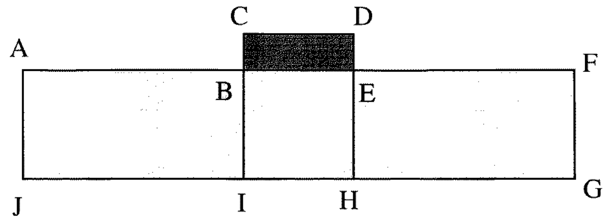

Figure 2. A strained overlayer can be modelled using several elastic blocks linked by appropriate interface conditions. The surface ABCDEFGHIJ is stress free, stress and displacement are continuous across BI and EH, but across BE the stress is continuous and the displacement and strain are discontinuous.

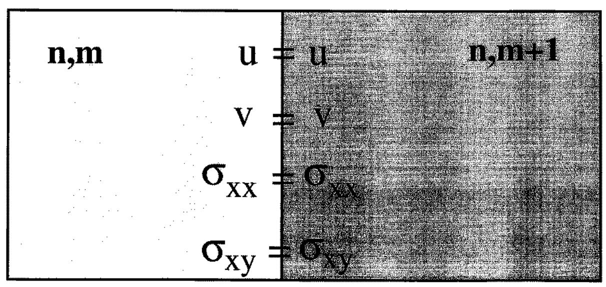

Figure 3. By using appropriate boundary conditions, two elastic blocks can be linked to form a single continuous elastic block.

figure 2 for instance). There may, however, be a discontinuity of strain and displacement across certain interfaces (across BE in figure 2 for instance), but the normal and shear stress are continuous across all interfaces in the material.

The first step is to calculate the strain state of a *single* rectangular block with either stress or displacement as specified boundary conditions. This involves taking the form for the stress function, as given by equation (3), finding expressions for the displacements at the boundary and equating these to the displacement boundary conditions in the same way as for stress described in the previous section. The analysis then proceeds in the manner described in section 2. First the stress components are determined from the stress function and the strain components are determined from the Hooke's laws assuming plane strain conditions. The displacements at the boundary $x = +\ell$, for example, are then obtained from the strains by

$$
\begin{aligned}
u(l, y) &= u(0, 0) + \int_0^l \epsilon_{xx}(x', 0)\, \mathrm{d}x' + \int_0^y \epsilon_{xy}(l, y')\, \mathrm{d}y' \\
v(l, y) &= v(0, 0) + \int_0^l \epsilon_{xy}(x', 0)\, \mathrm{d}x' + \int_0^y \epsilon_{yy}(l, y')\, \mathrm{d}y'
\end{aligned}
$$

where u and v are the displacements in the x and y directions, respectively, and the displacements at the origin of the local coordinates for this rectangle, $u(0, 0)$ and $v(0, 0)$, may be taken with respect to the centre of mass of the structure as a whole. For example, $u(l, y)$ is given by

$$u(l, y) = u(0,0) + \frac{1+\nu}{E}\left\{ \sum_{i=1}^{\infty} \frac{B_i^{\pm}}{\alpha_i'}[(1-\nu)h_i'^{\pm''}(0) + \alpha_i'^2 \nu h_i'^{\pm}(0)] \right.$$
$$+ \sum_{i=1}^{\infty} \frac{D_i^{\pm}}{\alpha_i'}[(1-\nu)i_i'^{\pm''}(0) + \alpha_i'^2 \nu i_i'^{\pm}(0)]$$
$$- \sum_{i=0}^{\infty} E_i^{\pm}\left[\beta_i^2(1-\nu)\int_0^l j_i^{\pm}(x)\,\mathrm{d}x + \nu \int_0^l j_i^{\pm''}(x)\,\mathrm{d}x\right]$$
$$- \sum_{i=0}^{\infty} G_i^{\pm}\left[\beta_i^2(1-\nu)\int_0^l k_i^{\pm}(x)\,\mathrm{d}x + \nu \int_0^l k_i^{\pm''}(x)\,\mathrm{d}x\right]$$
$$\left. + \sum_{i=0}^{\infty} \frac{G_i^{+}}{\beta_i}(1-\cos\beta_i y) - \frac{H_i^{+}}{\beta_i'}\sin\beta_i' y \right\}. \quad (13)$$

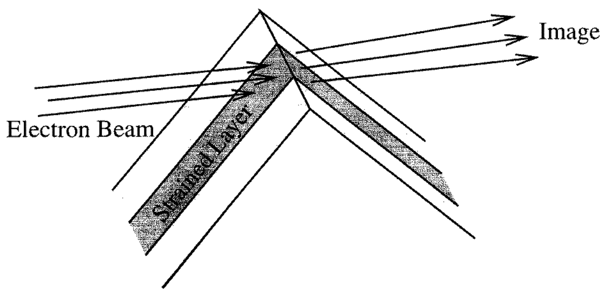

(*a*)

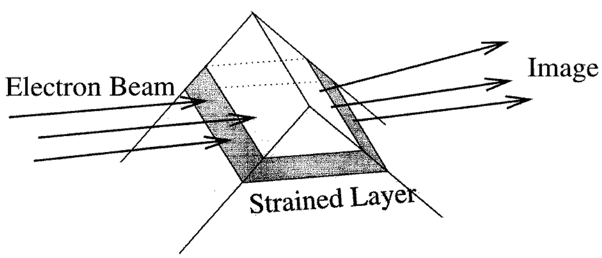

(*b*)

Figure 4. (*a*) The TEM sample studied by Harvey *et al* [7] and (*b*) the TEM sample studied by Chou [33].

These displacement relations can be used in the same way as equation (5) to generate a set of iteration equations relating the Fourier coefficients of the stress function, thereby allowing the strain field within a single rectangular elastic block with displacements specified as boundary conditions to be solved.

When solving for the strain distributions of two linked blocks, the boundary conditions are not known *a priori* at the interface. Instead the stress components and displacements at the interface of one block must equal those at the interface calculated from the stress function of the adjacent block. For example, for the two blocks shown in figure 3, the stress components and displacements at the right side of block (n, m) must be equal to those at

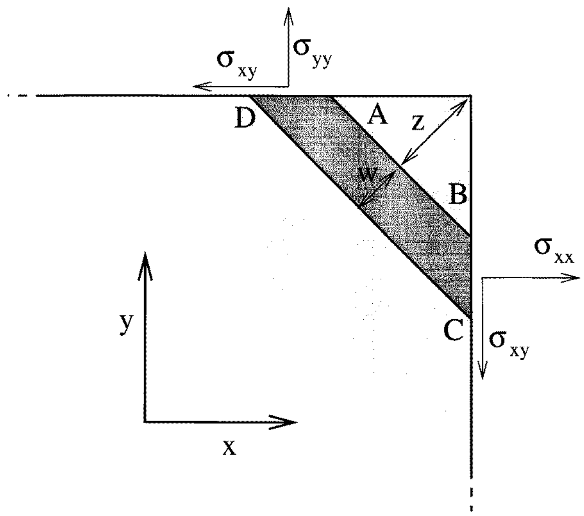

Figure 5. Geometry of the TEM sample, shown in figure 4(*b*), used in the strain calculation showing the boundary stresses used to calculate the strain relaxation.

the left side of block $(n,\ m+1)$. Therefore, for example, the continuity of the normal stress across the interface will yield

$$\sigma_{xx}(n, m, l_{n,m}) = \sigma_{xx}(n, m+1, -l_{n,m+1}) \tag{14}$$

where the subscripts on l indicate the block to which the dimension applies. Similar expressions apply for the shear stress and displacements. Thus, if the stress components and the displacements have been calculated for block $(n,\ m)$ based on a set of known or estimated boundary conditions, the stress components and the displacements at the boundary with block $(n,\ m+1)$ can be used as the first estimate of the boundary conditions (coupled with known or estimated boundary conditions on the remaining faces for block $(n,\ m+1)$. This technique, therefore, generates the stress at the interfaces without prior specification through fixed boundary conditions. This requires choosing Fourier frequencies (1) from table 1, because other choices result in iteration equations which are simplified to the extent that the stresses must be specified at the outset. With this proviso, it is possible, in principle, to use the Fourier-series method for more complex geometries.

4. Results

A TEM sample containing strained layers produces a different contrast pattern to a sample which is unstrained. The relaxation of the strain at a free surface causes bending of the atomic planes and this is detected by the curvature of thickness fringes [6–8]. The curvature of the thickness fringes is extremely sensitive to the magnitude of the strain relaxation and hence the bulk strain in strained-layer structures can be measured to high accuracy. These techniques are only useful, however, if accurate theoretical predictions for the strain relaxation are available.

One common sample geometry is the 90°-wedge sample with the normal to the plane of the strain layer running parallel to both surfaces [7], as shown in figure 4(*a*). The strain relaxation can be calculated using a three-dimensional analysis with boundary conditions

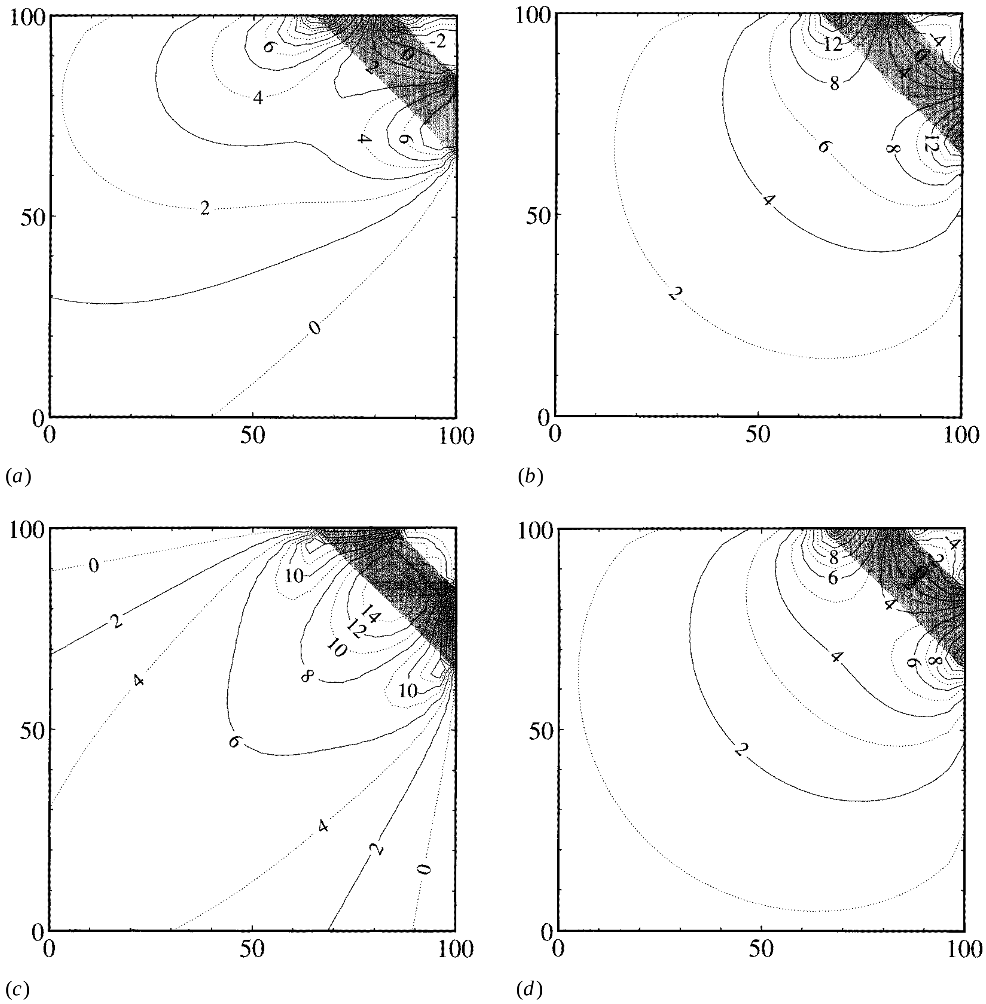

Figure 6. Contour plots of the stresses and strains of the TEM sample shown in figure 4. The dark shaded region shows the position of the strained layer. The absolute strain contours are labelled in units of 10^{-3} and the stress contours are labelled in units of 10^{7} N m^{-2}. (*a*) Normal stress (σ_{xx}), (*b*) in-plane stress ($\frac{1}{\sqrt{2}}(\sigma_{xx} + \sigma_{yy})$), (*c*) shear strain ($\epsilon_{xy}$) and (*d*) in-plane strain ($\frac{1}{\sqrt{2}}(\epsilon_{xx} + \epsilon_{yy})$). The distance scale is arbitrary.

consisting of stress components normal to the surfaces. A three-dimensional Fourier-series method has been developed for this purpose [17].

An alternative geometry has been investigated by Chou [33] for InGaAs strained layers in GaAs barriers. Here the normal to the plane of the strained layer is at 45° to both free surfaces of the sample, as shown in figure 4(*b*). If the wedge is thick enough, the strain relaxation for this sample can be calculated assuming plane strain conditions and is accessible to the theory outlined in section 2 for a single rectangular block. To establish a free surface, it is necessary that the stress *relaxation* cancels the in-plane stress of the layer at the surface. The stress relaxation is, therefore, calculated by applying normal and shear stress components at the surface as indicated in figure 5, where, for this calculation,

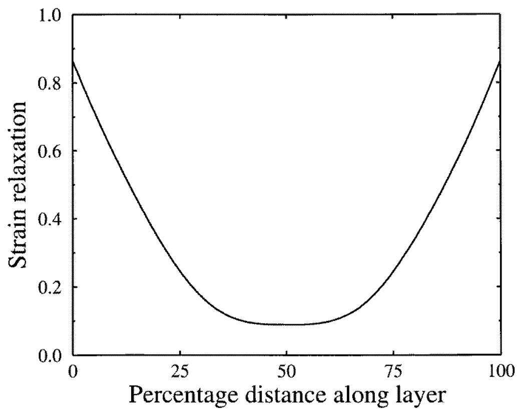

Figure 7. The relaxation of the in-plane strain along the centre of the layer for the TEM sample shown in figure 4(*b*).

z is equal to 10.6 and w is equal to 14.14. Note that the *actual* stress in the structure is obtained by taking the stress *relaxation* and adding the state of stress prior to relaxation.

Calculations of stress relaxation for the sample illustrated in figure 5 were performed using 500 Fourier frequencies and the strain fields were determined using the elastic constants for GaAs with $E = 8.5 \times 10^{10}$ N m^{-2} and $\nu = 0.312$ [34]. The misfit strain is taken to be 1% and results for other misfit strains can be scaled accordingly. It is a reasonable approximation to use the elastic constants of the barrier material for the layer because, as well as being known only approximately, the elastic constants for the III–V materials are roughly proportional to the lattice constant. The isotropic approximation of the Fourier series method is appropriate when the anisotropy factor $(c_{11} - c_{12})/2c_{44}$ is close to 1. For GaAs, this value is about 0.55, but earlier work suggests that the anisotropy of elastic constants makes only a small difference to the overall strain distribution [15].

The results for stress relaxation are shown in figure 6 as contour plots. The amount of relaxation of the in-plane strain is large at points A and B. This is expected because the layer is constrained by less material on the side AB than on the side CD. The relaxation of the in-plane strain along the centre of the layer is plotted as a function of distance in figure 7. As expected the strain is almost fully relaxed at the free surface. The strain at the centre of the layer has relaxed by about 0.1% and so the actual strain is about 0.9% in this region.

The in-plane stress is found to be approximately proportional to $1/r$, where r is the distance from the free surface. A $1/r$ dependence was noted by Faux [16] for a strained layer at right angles to the surface. For the TEM sample studied here, the stresses imposed at the two surfaces interact and so one would not expect an exact $1/r$ dependence.

5. Conclusion

The Fourier-series method for calculating the strain field in a two-dimensional rectangular isotropic elastic block is extended to include boundary conditions specified in terms of both normal and shear stresses. This method can be used to calculate quickly, to any desired accuracy, the state of stress and strain at any point within the block. In section 4, the method is used to calculate the strain field of a TEM sample. It is found that, for a strained layer close to the corner of a rectangular block and at 45° to the free surfaces, the in-plane stress is approximately proportional to $1/r$, where r is the distance from the free surface.

This strain field could be superposed to predict TEM contrast patterns and could, therefore, be combined with TEM measurements of thickness fringes to measure directly the misfit strain.

Finally, the further extension of the Fourier-series method to calculate the strain field due to buried inclusions or strained overlayers is presented. Separate rectangular blocks are linked to construct the more complex geometries, hence a Fourier-series method that allows displacements to be specified as boundary conditions is required and this theory is presented in section 3. This theory allows, in principle, calculations of stress and strain to be performed using the Fourier-series method in two-dimensional structures composed of rectangular elements. The increased mathematical complexity of the theory may, however, restrict its application to simple cases.

Acknowledgments

JRD acknowledges support of the Engineering and Physical Sciences Research Council (UK) through grant GR/K 81447.

References

[1] O'Reilly E P 1989 *Semicond. Sci. Technol.* **4** 121
[2] Grundmann M, Stier O and Bimberg D 1994 *Phys. Rev.* B **50** 14 187
[3] Christiansen S, Albrecht M, Strunk H P and Maier H J 1994 *Appl. Phys. Lett.* **64** 3617
[4] De Caro L and Tapfer L 1994 *Phys. Rev.* B **49** 11 127
[5] Hartman R L and Hartman A R 1973 *Appl. Phys. Lett.* **23** 147
[6] Chou C T, Anderson S C, Cockayne D J H, Sikorski A Z and Vaughan M R 1994 *Ultramicroscopy* **55** 334
[7] Harvey A J, Faux D A, Bangert U and Charsley P 1993 *Phil. Mag.* A **67** 433
[8] Treacy M M J and Gibson J M 1986 *J. Vac. Sci. Technol.* B **4** 1458
[9] Faux D A, Howells S G, Bangert U and Harvey A J 1994 *Appl. Phys. Lett.* **64** 1271
[10] Harker A H, Pinardi K, Jain S C, Atkinson A and Bullough R 1995 *Phil. Mag.* A **71** 871
[11] Banerjee P K 1994 *Boundary Element Methods in Engineering* (London: McGraw-Hill)
[12] Cembali F and Servidori M 1989 *J. Appl. Cryst.* **22** 345
[13] Chiu Y P 1978 *J. Appl. Mech.* **45** 302
[14] Downes J R and Faux D A 1994 *J. Appl. Phys.* **77** 2444
[15] Faux D A and Haigh J 1990 *J. Phys.: Condens. Matter* **2** 10 289
[16] Faux D A 1994 *J. Appl. Phys.* **75** 186
[17] Faux D A and Gill J 1994 *J. Appl. Phys.* **75** 4963
[18] Feng Z and Liu H 1983 *J. Appl. Phys.* **54** 83
[19] Fischer A 1983 *Crystal Res. Technol.* **18** 1415
[20] Fischer A and Richter H 1992 *Appl. Phys. Lett.* **61** 2656
[21] Fischer A and Richter H 1994 *J. Appl. Phys.* **75** 657
[22] Glas F 1991 *J. Appl. Phys.* **70** 3556
[23] Gosling T J and Willis J R 1995 *J. Appl. Phys.* **77** 5601
[24] Hu S M 1978 *Appl. Phys. Lett.* **32** 5
[25] Hu S M 1979 *J. Appl. Phys.* **50** 4661
[26] Nakajima K 1992 *J. Appl. Phys.* **72** 5213
[27] Nishi K, Yamaguchi A A, Ahopelto J, Usui A and Sakaki H 1994 *J. Appl. Phys.* **76** 7437
[28] Olsen G H and Ettenberg M 1977 *J. Appl. Phys.* **48** 2543
[29] Saul R H 1969 *J. Appl. Phys.* **40** 3273
[30] Suhir E 1986 *J. Appl. Mech.* **53** 657
[31] Pickett G 1944 *J. Appl. Mech.* **A** 176
[32] Timoshenko S P and Goodier J N 1970 *Theory of Elasticity* (New York: McGraw-Hill)
[33] Chou C T private communication
[34] Fitzgerald E A 1993 *EMIS Data Review Series No 8: Properties of Lattice-Matched and Strained Gallium Arsenide* (London: INSPEC-IEE) p 6